

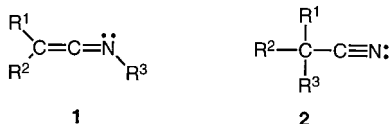
## Desulfurization of 4-Nitro-*N*,2-diphenyl-3-(phenylamino)isothiazol-5(2*H*)-imine: Formation of a 3-Imino-2-nitroprop-2-enamidine<sup>1)</sup>

by Dally Moya Argilagos<sup>2)</sup>, Roland W. Kunz, Anthony Linden, and Heinz Heimgartner\*

Organisch-chemisches Institut der Universität Zürich, Winterthurerstrasse 190, CH-8057 Zürich

The course of the desulfurization reaction of 4-nitro-*N*,2-diphenyl-3-(phenylamino)isothiazol-5(2*H*)-imine (**3**) is investigated and the formation of the unstable 3-imino-2-nitroprop-2-enamidine (**A**) as intermediate is discussed. Addition of amines and thiophenol to the reaction mixture yielded the amidine derivatives **5** and the thioimidate **6**, respectively, *via* nucleophilic addition of the respective reagent to **A** (*Scheme 2*). Benzoic acid and thiobenzoic acid afforded the amide **7** and the thioamide **8**, respectively, as secondary products of the expected adducts **7a** and **8a** (*Schemes 3* and *4*). The presence of (benzylidene)(methyl)amine in the reaction mixture of the desulfurization of **3** led to the 1,2,4-oxadiazole derivative **10**, together with the quinoxaline *N*-oxide **4** as a minor product. Reaction mechanisms involving an intermediate ketene imine and participation of the NO<sub>2</sub> group in the reaction leading to 1,2,4-oxadiazole **10** are proposed. *Ab initio* calculations of model structures for the nitroketene imine were performed and the results correlated with the experimental results. The structures of **8** and **10** were established by X-ray crystal-structure analysis.

**1. Introduction.** – Ketene imines **1** have attracted considerable interest as substrates in organic synthesis [1–3], especially for the synthesis of heterocycles [4–7], where cycloaddition reactions are mainly involved [8–13]. Moreover, recent studies of the rearrangement of intermediate *N*-allylketene imines (**1**, R<sup>3</sup> = CH<sub>2</sub>=CHCH<sub>2</sub>) to give the isomeric nitriles **2** have indicated new applications of the ketene-imine chemistry [14–16].

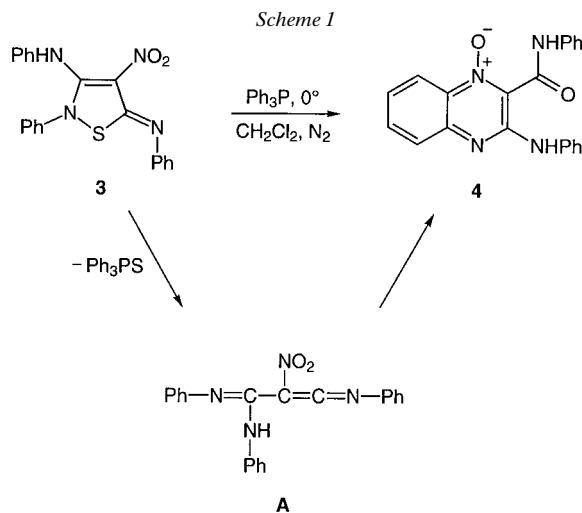


Ketene imines were first prepared by *Staudinger* in unspecified yield by the interaction of a phosphinimine with a ketene [17]. Since then, several methods for their preparation have been described [18] such as alkylation of nitrile derivatives, addition of isocyanides to alkynes and to carbenes, reaction of nitrile oxides with phosphorylides, dehydration of amides [19], and reaction of nitrilium salts with an organic base [20], among others. The desulfurization of S-containing compounds such as thioureas [21][22], thioamides [5][23][24], thioimidates [25][26], dithioles [27], thiadiazoles, and isothiazoles [28][29] leads also to the formation of ketene imines. Recently, we have reported on the desulfurization of 3,3-diamino-2-nitroprop-2-enethioamides which yields nitroketene imines as reactive intermediates [26][30][31].

<sup>1)</sup> Presented in part at the 36th IUPAC Congress, Geneva, Switzerland, August 1997.

<sup>2)</sup> Part of the Ph.D. thesis of *D.M.A.*, Universität Zürich, 1998.

The synthesis of alkene-diimines (**1**,  $R^2 = RC(NR')$ ) by S-extrusion from isothiazole derivatives with  $Ph_3P$  [28][29] prompted us to investigate the desulfurization of the nitroisothiazol derivative **3**, which was expected to yield 3-imino-2-nitroprop-2-enamidine **A** as a useful intermediate for the synthesis of  $NO_2$ -substituted compounds. However, upon treatment of **3** with  $Ph_3P$ , the quinoxaline *N*-oxide **4** (*Scheme 1*) and numerous decomposition compounds were obtained (*cf.* [32]).



Taking into account the formation of **4** and the occurrence of two bands at 2337 and 2261  $cm^{-1}$  in the IR spectra of the crude reaction mixture, which disappeared under the reaction conditions (*cf.* [32]), the presence of a highly reactive intermediate ketene imine, which undergoes cyclization and decomposition could be suggested. In the present paper, we report on the attempts to confirm this proposal by trapping the reactive intermediate with nucleophiles. In addition, *ab initio* calculations of model structures of **A** were carried out to evaluate the influence of the  $NO_2$  group (*cf.* **A**; *Scheme 1*) and the contribution of a mesomeric nitrilium form to the ketene-imine structure, which could explain the shift of the observed IR bands compared with those of known ketene imines (*ca.* 2000  $cm^{-1}$ ).

**2. Results.** – 2.1. *Formation of 2-Nitro-N²-phenyl-3,3-bis(phenylamino)prop-2-enamidines 5.* The desulfurization of 4-nitroisothiazol-5(2*H*)-imine **3** with  $Ph_3P$  at 0° [31][32] in the presence of different amines (*Method A*) led to the corresponding 2-nitro-propenamidines **5** in good yields (*Scheme 2* and *Table I*). On the other hand, when morpholine and pyrrolidine were added after completion of the reaction of **3** with  $Ph_3P$  (TLC monitoring), derivatives **5a** and **5b** were isolated (*Method B*) as well as 4% quinoxaline *N*-oxide **4** (*cf.* [32]), but some decomposition products were also formed. The proposed mechanism of the reaction involves the formation of an intermediate ketene imine **A** followed by nucleophilic attack by the amine. Thus, the presence of an amine in the reaction mixture led only to the adduct **5**, while amine addition, after the desulfurization step, resulted in the additional formation of

quinoxaline *N*-oxide **4** and decomposition products of intermediate **A**. Therefore, *Method B* led to lower yields of **5** compared with *Method A*. Moreover, the IR bands observed in the reaction mixture of the desulfurization of **3** were only detected in the absence of amines (*Method B*), disappearing immediately after amine addition.

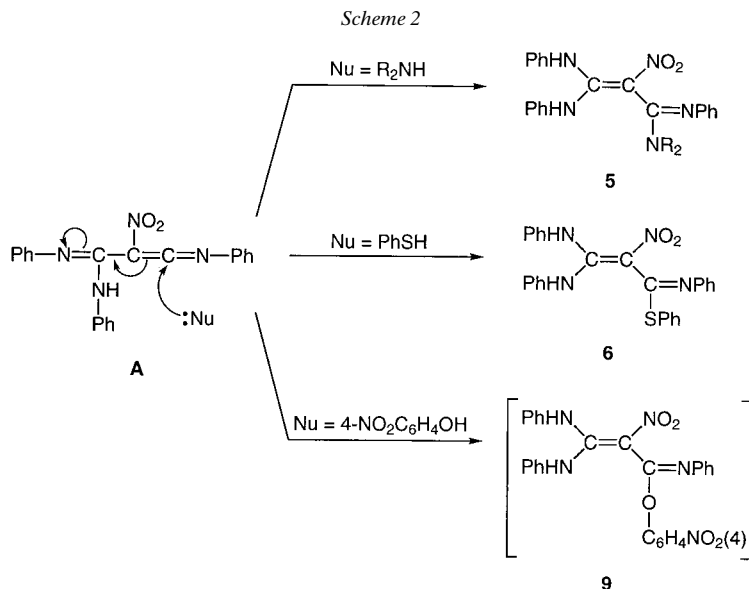


Table 1. Prepared 2-Nitro-*N*<sup>2</sup>-phenyl-3,3-bis(phenylamino)prop-2-enamidines **5**

Compound	R,R	Yield [%] <sup>a)</sup>	
		<i>Method A</i>	<i>Method B</i>
<b>5a</b>	–(CH <sub>2</sub> ) <sub>2</sub> O(CH <sub>2</sub> ) <sub>2</sub> –	99	90
<b>b</b>	–(CH <sub>2</sub> ) <sub>4</sub> –	93	72 <sup>b)</sup>
<b>c</b>	Et, Et	91	–
<b>d</b>	PhCH <sub>2</sub> , H	76 <sup>b)</sup>	–

<sup>a)</sup> With respect to **3**. <sup>b)</sup> Isolation of the compounds was particularly difficult.

The 2-nitro-*N*<sup>2</sup>-phenyl-3,3-bis(phenylamino)prop-2-enamidines **5** were purified by flash column chromatography and characterized by their spectroscopic data. Although, according to TLC, the reactions following *Method A* led exclusively to the formation of **5** and Ph<sub>3</sub>PS, the yield of isolated **5** was only 72–93%. As an exception, **5a** was obtained quantitatively (*Table 1*).

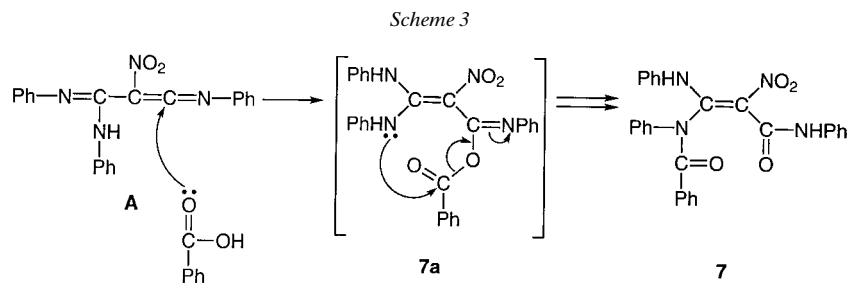
The <sup>1</sup>H- and <sup>13</sup>C-NMR spectra of compounds **5** in (D<sub>6</sub>)DMSO as well as in CDCl<sub>3</sub> at room temperature show, in general, quite broad signals for the H- and C-atoms. This observation, in addition to the equivalence of the two NH groups in the <sup>1</sup>H-NMR spectra, indicate a slow interconversion of conformers by rotation around the C–N(amino) bonds, as is usually found for similar push-pull compounds [26][33]. In addition, a rotation around the formal C(2)=C(3) bond must also take place (*cf.* [30]).

Surprisingly, aniline and 4-methoxyaniline did not react in the expected fashion, and the reaction behavior in these cases was analogous to that observed when no amines were added to the mixture<sup>3</sup>). To evaluate the influence of the nucleophilic reagent, the reactions were carried out with other nucleophiles.

2.2. *Formation of Phenyl 2-Nitro-N-phenyl-3,3-bis(phenylamino)prop-2-enethioimidate (6)*. In accordance with the results mentioned in *Sect. 2.1*, the addition of PhSH after the desulfurization of **3** (*Method B*) yielded the phenyl thioimidate **6** via nucleophilic attack of PhSH to the intermediate **A** (*Scheme 2*). IR Monitoring of the reaction showed again the disappearance of the characteristic IR absorptions assigned to **A** after the addition of PhSH. Very surprisingly, BuSH, PrSH, and i-PrSH did not yield any addition products; the reactions led only to decomposition compounds and quinoxaline *N*-oxide **4**, as in the absence of nucleophilic reagents.

The phenyl thioimidate **6** was isolated, after column chromatography, in 62% yield as well as quinoxaline *N*-oxide **4** (4%) and Ph<sub>3</sub>PS (95%), and characterized spectroscopically. The broad signals in the <sup>1</sup>H- and <sup>13</sup>C-NMR spectra of **6** in CDCl<sub>3</sub> at room temperature point once more to slow interconversion of the conformers<sup>4</sup>). Indeed, the <sup>1</sup>H-NMR spectrum in (D<sub>6</sub>)DMSO at room temperature shows, besides signals for the aromatic H-atoms, the presence of three down-field-shifted signals corresponding to the NH-atoms of different conformers. In the <sup>13</sup>C-NMR spectrum in (D<sub>6</sub>)DMSO at room temperature, only very broad signals were observed.

2.3. *Formation of N-[2-Nitro-1-(phenylamino)-2-(N-phenylcarbamoyl)ethenyl]-N-phenylbenzamide (7)*. Addition of PhCOOH to the reaction mixture from the desulfurization of **3** led to the unexpected benzamide **7** (*Scheme 3*). A reaction mechanism via nucleophilic addition of PhCOOH to the intermediate **A** yielding the unstable benzoate **7a**, and subsequent intramolecular *N*-acylation could explain the formation of the more stable **7**.



The amide **7** was obtained in 67% yield after purification by column chromatography, and it was characterized by its spectroscopic data using principally 2D-NMR spectroscopy.

The <sup>1</sup>H-NMR spectrum in CD<sub>3</sub>CN at 220 K exhibits, besides the signals for the aromatic H-atoms, two down-field-shifted signals at 9.11 and 11.29 ppm assigned to the

<sup>3</sup>) The same results were observed by carrying out the reaction in MeOH: Ph<sub>3</sub>PS and quinoxaline *N*-oxide **4** precipitated from the reaction mixture, but no adduct of the ketene imine with MeOH was detected.

<sup>4</sup>) A possible rotation around the formal C(2)=C(3) bond is supported by the bond lengths in the crystal structure of a corresponding methylthio derivative reported in [26].

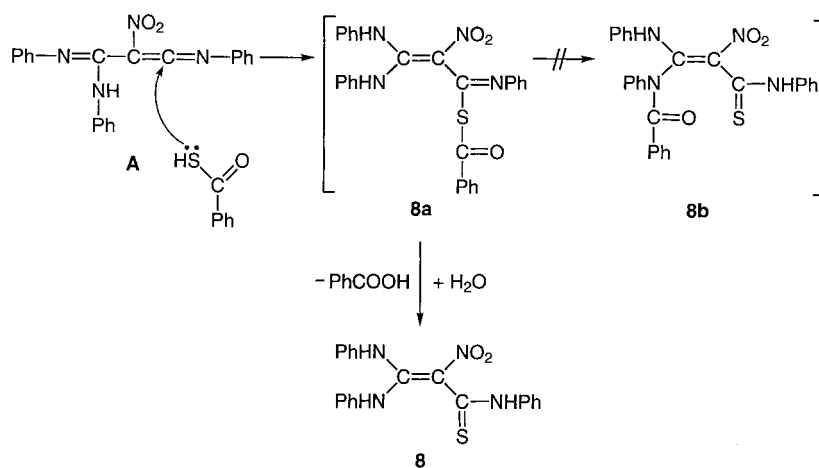
*NH*-atom of the PhNH and that of the carbamoyl group, respectively. The HMBC spectrum recorded under the same conditions shows for both *NH* groups correlation peaks, which are in accordance with the proposed structure. The *NH* appearing at 9.11 ppm exhibits a cross-peak with the *ortho*-C-atoms of a Ph ring ( $^3J(\text{C,H})$ ) and, in addition, shows a  $^2J(\text{C,H})$  correlation with the corresponding aromatic C(1)-atom, confirming the presence of the PhNH group. A second  $^2J(\text{C,H})$  cross-peak indicates a further coupling of this *NH* with C(3). The *NH* arising at 11.29 ppm displays two cross peaks, indicating the corresponding  $^3J(\text{C,H})$  and  $^2J(\text{C,H})$  correlation with a Ph ring. Additionally, a  $^3J(\text{C,H})$  cross-peak to the C-atom bearing the NO<sub>2</sub> group and a  $^2J(\text{C,H})$  cross-peak to a C=O group appeared. These data confirmed that the two PhNH groups are not attached to the same C-atom and indicated the presence of benzamide structure **7**, ruling out the alternative structure **7a**. In addition, the low-field shift of one of the *NH* resonances could be explained due to the deshielding effect of the C=O group of the benzamide group.

Broad signals in the <sup>1</sup>H- and <sup>13</sup>C-NMR spectra of **7** in CD<sub>3</sub>CN at room temperature hint again at an equilibrium between several conformers. This assumption was confirmed by low-temperature NMR experiments which clearly exhibited splitting of the *NH* signal at 9.11 ppm due to the freezing of the conformations.

2.4. Formation of 2-Nitro-N-phenyl-3,3-bis(phenylamino)prop-2-enethioamide (**8**). In contrast to the results described in Sect. 2.3, addition of PhCOSH to the reaction mixture from the desulfurization of **3** led to the isolation of the thioamide **8**, instead of the expected adduct **8a** or the *N*-acylated product **8b** (Scheme 4). The formation of **8** can be explained by the hydrolysis of **8a**, formed by the nucleophilic addition of PhCOSH to **A**, in analogy to the already described addition of amines and PhCOOH (cf. Sect. 2.1 and 2.3, resp.). Since the reaction was performed under anhydrous conditions, hydrolysis of **8a** must have resulted from the column chromatography on silica gel during workup.

The thioamide **8** was isolated in 75% yield and characterized spectroscopically. Its properties were identical with those of **8** obtained by another route [34]. After

Scheme 4



crystallization from MeOH, the structure of **8** was established by X-ray crystallography (Fig. 1).

The crystal structure of **8** revealed that the asymmetric unit contains two molecules (A and B) and a partially occupied site for a H<sub>2</sub>O molecule. The molar amount of H<sub>2</sub>O in the structure is *ca.* 10%. The two independent molecules differ most significantly in

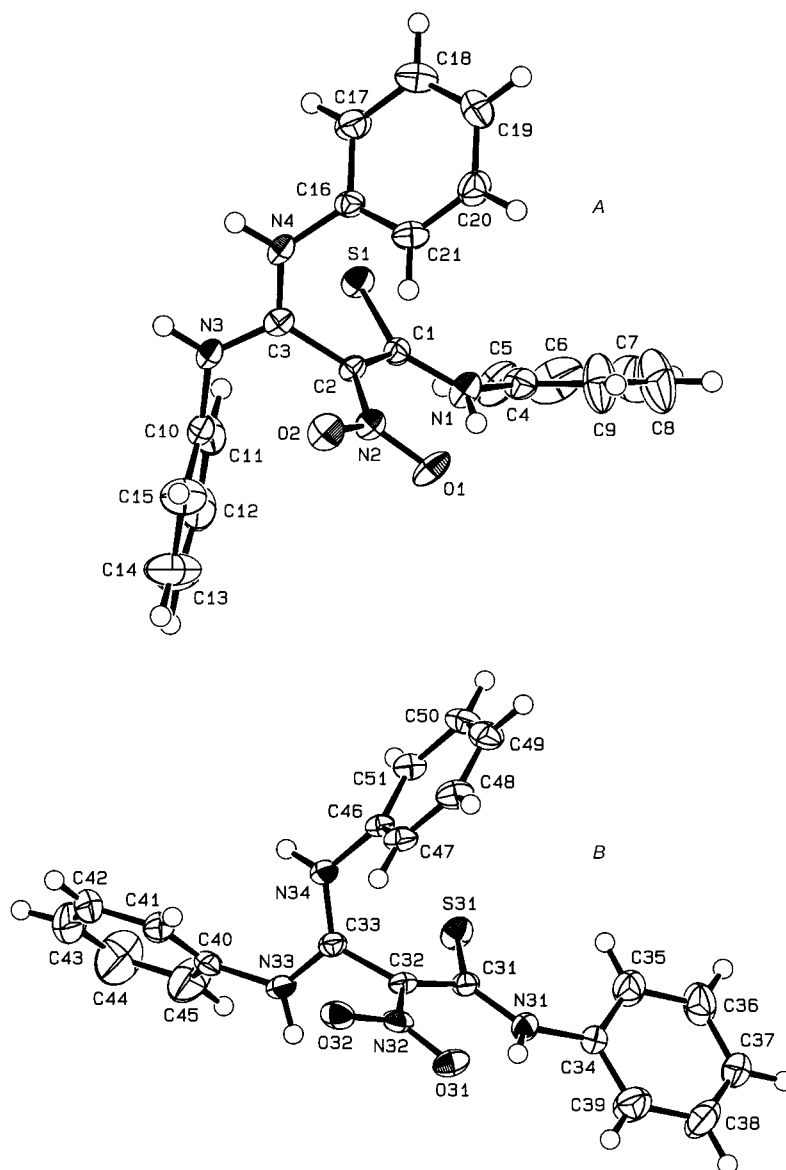


Fig. 1. ORTEP Plot [35] of the molecular structures of the two independent molecules A and B of **8** (arbitrary numbering of the atoms, with 50% probability ellipsoids)

the orientation of one PhNH group, which is rotated by *ca.* 175°, but there are also slight differences in the orientations of the other Ph rings. The structure shows the usual non-planarity across the C(2)–C(3)<sup>5</sup> bond (*cf.* [26][30]), with the planes on either side of the C(2)–C(3) bond making angles of 81.5(3) and 83.1(3)° for molecules *A* and *B*, respectively. Note that all atoms in each of the regions C(4) to N(2), and C(10) to C(16) form highly planar systems, which suggest  $\pi$ -bonding delocalization in these regions (*cf.* [30]). This is supported by the corresponding bond lengths, which again show the usual patterns (*Table 2*).

Table 2. Selected Bond Lengths [Å] and Torsion Angles [°] for Molecules *A* and *B* of **8** (*cf.* Fig. 1)

Molecule <i>A</i>				Molecule <i>B</i>					
S(1)–C(1)	1.690(4)	N(1)–C(1)	1.330(5)	S(31)–C(31)	1.671(4)	N(31)–C(31)	1.348(4)		
C(1)–C(2)	1.436(5)	N(2)–C(2)	1.360(4)	C(31)–C(32)	1.457(5)	N(32)–C(32)	1.339(4)		
C(2)–C(3)	1.490(5)	N(3)–C(3)	1.317(5)	C(32)–C(33)	1.486(5)	N(33)–C(33)	1.321(5)		
N(4)–C(3)	1.313(5)			N(34)–C(33)	1.320(5)				
S(1)–C(1)–N(1)–C(4)				0.1(6)	S(31)–C(31)–N(31)–C(34)				1.1(6)
C(2)–C(1)–N(1)–C(4)				–179.1(4)	C(32)–C(31)–N(31)–C(34)				–179.6(4)
N(1)–C(1)–C(2)–C(3)				176.4(4)	N(31)–C(31)–C(32)–C(33)				–173.1(3)
N(1)–C(1)–C(2)–N(2)				–4.7(6)	N(31)–C(31)–C(32)–N(32)				–0.9(6)
S(1)–C(1)–C(2)–C(3)				–2.9(5)	S(31)–C(31)–C(32)–C(33)				6.3(5)
S(1)–C(1)–C(2)–N(2)				176.0(3)	S(31)–C(31)–C(32)–N(32)				178.5(3)
O(1)–N(2)–C(2)–C(1)				0.6(6)	O(31)–N(32)–C(32)–C(31)				1.8(6)
O(1)–N(2)–C(2)–C(3)				179.6(3)	O(31)–N(32)–C(32)–C(33)				174.3(3)
O(2)–N(2)–C(2)–C(1)				179.1(3)	O(32)–N(32)–C(32)–C(31)				–179.0(3)
O(2)–N(2)–C(2)–C(3)				–1.9(5)	O(32)–N(32)–C(32)–C(33)				–6.6(5)
C(1)–C(2)–C(3)–N(3)				99.4(4)	C(31)–C(32)–C(33)–N(33)				93.4(4)
C(1)–C(2)–C(3)–N(4)				–80.2(5)	C(31)–C(32)–C(33)–N(34)				–86.3(5)
C(2)–C(3)–N(4)–C(16)				0.9(6)	C(32)–C(33)–N(34)–C(46)				–0.9(6)
C(2)–C(3)–N(3)–C(10)				–4.8(6)	C(32)–C(33)–N(33)–C(40)				179.4(4)
N(2)–C(2)–C(3)–N(3)				–79.7(5)	N(32)–C(32)–C(33)–N(33)				–79.8(5)
N(2)–C(2)–C(3)–N(4)				100.7(4)	N(32)–C(32)–C(33)–N(34)				100.5(4)
N(3)–C(3)–N(4)–C(16)				–178.7(4)	N(33)–C(33)–N(34)–C(46)				179.5(4)
N(4)–C(3)–N(3)–C(10)				174.8(4)	N(34)–C(33)–N(33)–C(40)				–0.9(7)

In molecule *A*, H–N(1) of the thioamide group forms an intramolecular H-bond with O(1) of the NO<sub>2</sub> group (graph set: S(6) [36]; N⋯O 2.637(4) Å, N–H⋯O 141(3)°), forming a six-membered ring. Molecule *B* forms an identical intramolecular H-bond (N⋯O 2.634(4) Å, N–H⋯O 142(4)°). Additionally, H–N(3) of molecule *A* forms weak bifurcated intermolecular H-bonds with both of the O-atoms of the NO<sub>2</sub> group of molecule *B* (N⋯O 3.346(4) and 3.087(4) Å, N–H⋯O 165(3)° and 134(3)°, resp.), and H–N(33) of molecule *B* interacts, in an identical fashion, with a different molecule *A* (N⋯O 3.147(4) and 3.007(4) Å, N–H⋯O 151(4)° and 146(4)°, resp.). This links the molecules into cyclic ⋯*A*⋯*B*⋯*A*⋯*B*⋯ centrosymmetric tetramers; graph sets: R<sub>1</sub><sup>2</sup>(4) for the local interaction and R<sub>4</sub><sup>4</sup>(24) for the tetramer. H–N(4) of molecule *A* also forms bifurcated intermolecular H-bonds, one being with O(32) of the NO<sub>2</sub> group (N⋯O 2.802(4) Å, N–H⋯O 156(3)°) of the same molecule *B* as above; graph set: D, while the other weaker interaction is with O(2) of the NO<sub>2</sub> group (N⋯O

<sup>5</sup>) The arbitrary numbering of the atoms in the ORTEP diagram (*Fig. 1*) is used.

2.923(4) Å, N–H···O 108(3)°) of a neighboring molecule *A*. This latter interaction forms centrosymmetric ···*A*···*A*··· dimers; graph set: R<sub>2</sub><sup>2</sup>(12) [36]. Molecule *B* does not have the latter two interactions. Instead, H–N(34) forms an intermolecular H-bond with the S-atom of the C=S group (N···S 3.220(4) Å, N–H···S 152(3)°) of molecule *A*; graph set: D. This difference is presumably brought about by the 175° difference in the torsion angles about the C(3)–N(3) and the C(33)–N(33) bonds (Table 2). The combination of all intermolecular interactions links the molecules into an infinite two-dimensional network which lies perpendicular to the [101] direction.

2.5. *Formation of 4-Nitrophenyl 2-Nitro-N-phenyl-3,3-bis(phenylamino)prop-2-enimidate (9)*. Addition of 4-nitrophenol to the reaction mixture from the desulfurization of **3** induced a similar reaction course (TLC and IR monitoring) as already observed by the addition of amines (*cf. Sect. 2.1*). TLC indicated the presence of a main product besides Ph<sub>3</sub>PS and traces of the quinoxaline *N*-oxide **4**. Nevertheless, the expected adduct **9** could not be isolated since it decomposed during workup *via* flash column chromatography. Attempts to isolate **9** under different conditions led only to a small amount of impure **9** which was characterized by mass spectrometry. The ESI-MS exhibits a strong peak corresponding to [*M* + H] of the expected product, but the molecular weight and the similarity of the reaction courses of the formation of **5** and **6** with that of **9** were the only evidences for structure **9**.

2.6. *Formation of 4,5-Dihydro-4-methyl-N<sup>1</sup>,N<sup>2</sup>,5-triphenyl-1,2,4-oxadiazole-3-carbamidine (10)*. In the presence of (benzylidene)(methyl)amine (*Method A*), the desulfurization of **3** afforded a new addition product characterized as the 1,2,4-oxadiazole derivative **10**. A completely novel and unprecedented reaction mechanism for its formation is proposed in *Scheme 5*: after nucleophilic attack of an O-atom of the NO<sub>2</sub> group at the electrophilic C-atom of **A**, a formal 1,3-dipolar cycloaddition with the (benzylidene)(methyl)amine leads to a bicyclic adduct which, by elimination of phenylisocyanate, yields **10**. A *retro*-cycloaddition of the oxazetine *N*-oxide to give phenyl isocyanate and a nitrile oxide, which then undergoes a 1,3-dipolar cycloaddition with the imine, is conceivable as well. The participation of the NO<sub>2</sub> group in this mechanism is in accordance with the reaction pattern of the nitroketene imine observed in the desulfurization of 4-nitroisothiazol-5(2*H*)-imines **3** in the absence of trapping reagents [32]. As a side product, the quinoxaline *N*-oxide **4** was detected in minor amounts.

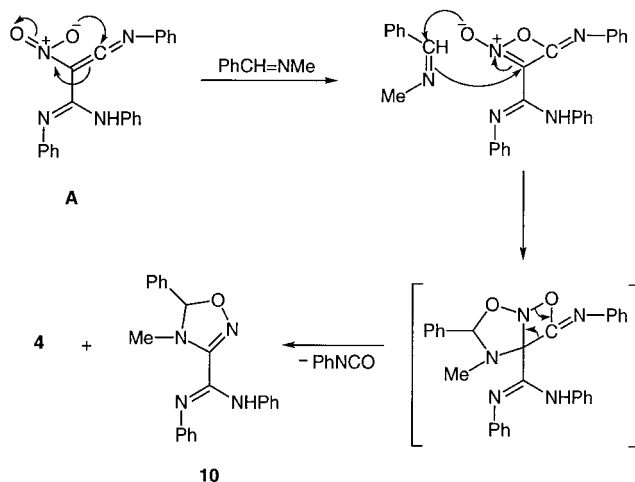
The 1,2,4-oxadiazole **10** was obtained in 36% yield after purification by MPLC. Attempts to elucidate the structure by 2D-NMR spectroscopy failed due to the absence of <sup>3</sup>*J*(C,H) correlation peaks to the nonaromatic sp<sup>2</sup> C-atoms in the HMBC spectrum. Therefore, the assignment of the signals could be achieved only partially. After crystallization of the material from MeOH, the structure of **10** was established by X-ray crystallography (*Fig. 2*).

The molecules of **10** crystallize in a chiral space group. However, the asymmetric unit contains two symmetry-independent molecules (*A* and *B*) which are enantiomorphs. Therefore, the crystals are racemic, and the direction of the polar axis in the crystal lattice has been chosen arbitrarily. The two molecules are practically mirror images of one another, although the Ph ring at C(2)<sup>6</sup> in molecule *A* is rotated by *ca.*

<sup>6</sup>) The arbitrary numbering of the atoms in the ORTEP diagram (*Fig. 2*) is used.



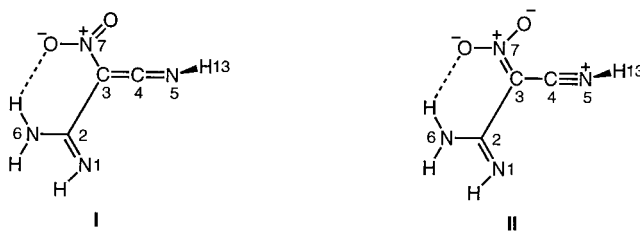
Scheme 5



$13^\circ$  with respect to its orientation in molecule **B**. Tests showed that the molecules were not related by any additional symmetry from a higher symmetry space group. The pseudo-mirror relating the molecules is also not parallel to any of the unit cell axes.

The amino group of each symmetry independent molecule forms an intermolecular H-bond with the unsubstituted N-atom of the oxadiazole ring ( $\text{N}\cdots\text{N}$  2.935(6) and 2.968(6) Å,  $\text{N-H}\cdots\text{N}$  154(4) $^\circ$  and 156(5) $^\circ$ , in molecules **A** and **B**, resp.) of a neighboring symmetry unrelated molecule. The interactions link the molecules into infinite one-dimensional  $\cdots A \cdots B \cdots A \cdots B \cdots$  chains which run parallel to the  $x$ -axis; graph set:  $\text{C}_2^2(10)$ .

**3. Molecular-Structure Calculations.** – *Ab initio* calculations at the 6-31G\*/MP2 level of the ketene-imine structure **I** and the nitrilium structure **II** indicate that they represent mesomeric forms from which only **I** exists. This is clearly shown by the optimized geometry of the **I**.



As a starting geometry for the calculations, the structure of the nitrilium derivative **II** was assumed. Optimization of the geometry of different conformations (torsion angle of the  $\text{C}(2)–\text{C}(3)$  bond and (*E*)/(*Z*) variation of the  $\text{N}(1)–\text{C}(2)$  bond) afforded stable gas-phase conformations within an energy range of 3.5 kcal/mol. They all possess the ketene-imine structure **I** with the lowest energy. The geometrical properties of **I** are summarized in *Table 3*.

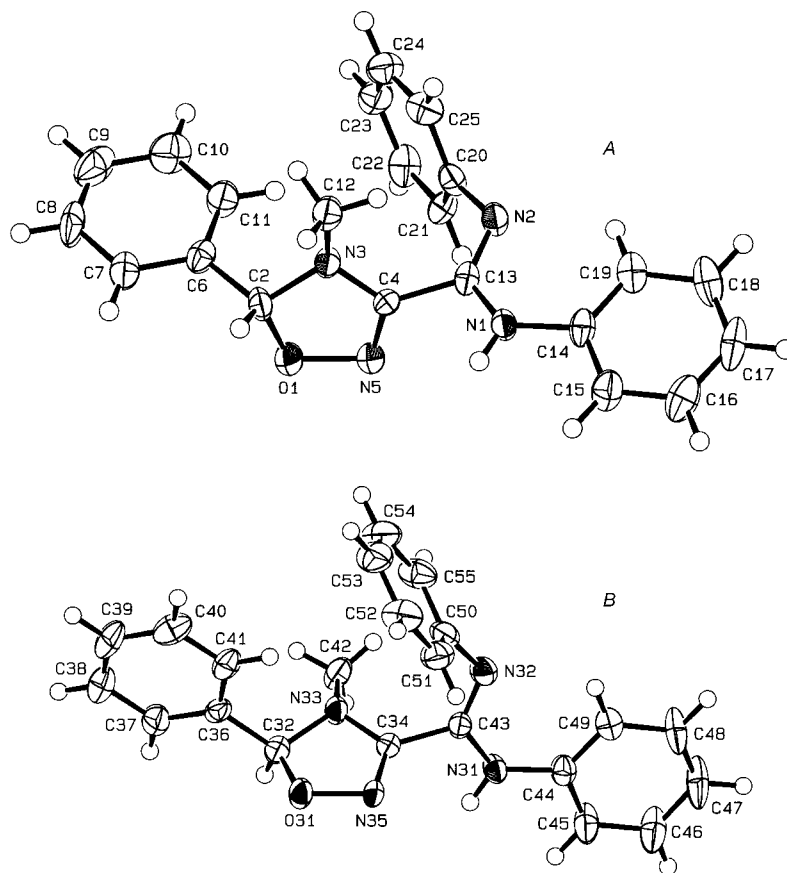


Fig. 2. ORTEP Plot [35] of the molecular structures of the two independent molecules A and B of **10** (arbitrary numbering of the atoms, with 50% probability ellipsoids)

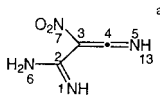
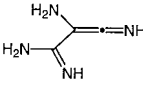
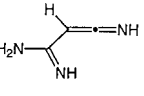
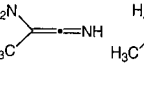
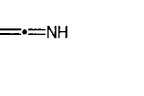
Table 3. Calculated Bond Lengths [Å], and Bond and Torsion Angles [°], and H-Bond [Å] for **1**

N(1)–C(2)	1.293	N(1)–C(2)–C(3)	114.5
C(2)–C(3)	1.485	C(2)–C(3)–C(4)	118.5
C(2)–N(6)	1.378	C(2)–C(3)–N(7)	126.4
C(3)–C(4)	1.343	C(3)–C(4)–N(5)	170.9
C(3)–N(7)	1.438	C(4)–N(5)–N(13)	124.2
C(4)–N(5)	1.213		
N(5)–N(13)	1.019		
N(1)–C(2)–C(3)–C(4)		–17.0	
C(2)–C(3)–N(5)–H(13)		86.0	
N(6)H⋯O		2.007	

For a detailed investigation of the bond relations in the molecule, a series of ketene imines and comparable structures were calculated *ab initio* (6-31G\*/MP2) yielding bond lengths, bond orders, and torsion angles which are given in *Tables 4* and *5*. The

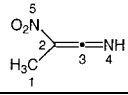
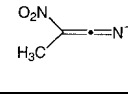
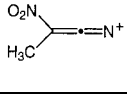
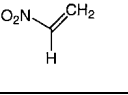
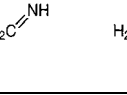
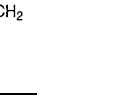
observed changes of the charge distribution in the molecules upon modification of the substitution pattern are presented in *Table 6*.

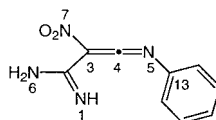
Table 4. *Calculated Bond Lengths [Å] (bond orders) and Torsion Angles [°] for Substituted Ketene Imines*

					
Bond lengths [Å] (bond orders)					
N(1)–C(2)	1.293(1.75)	1.292(1.76)	1.290(1.77)	–	–
C(2)–C(3)	1.485(0.93)	1.480(0.98)	1.472(0.96)	1.495(0.94)	1.507(0.91)
C(2)–N(6)	1.378(1.03)	1.387(1.01)	1.399(0.97)	–	–
C(3)–C(4)	1.343(1.43)	1.333(1.55)	1.327(1.65)	1.332(1.53)	1.319(1.75)
C(3)–N(7)	1.438(0.82)	1.437(0.94)	1.085(0.87)	1.446(0.83)	1.087(0.88)
C(4)–N(5)	1.213(1.94)	1.237(1.85)	1.231(1.89)	1.227(1.88)	1.243(1.85)
N(5)–H(13)	1.019(0.75)	1.025(0.77)	1.023(0.76)	1.023(0.75)	1.025(0.78)
Bond angles [°]					
N(1)–C(2)–C(3)	114.5	118.8	119.9		
C(2)–C(3)–C(4)	118.5	119.0	119.8		
C(2)–C(3)–N(7)	126.4	118.5	120.8		
C(3)–C(4)–N(5)	170.9	168.3	172.4		
C(4)–N(5)–H(13)	124.2	115.8	117.1		
Torsion angles [°]					
N(1)–C(2)–C(3)–C(4)	– 17.0	– 7.8	– 18.9		
C(2)–C(3)–C(4)–H(13)	86.0	88.0	87.6		

<sup>a)</sup> The same numbering of the atoms is used for all the structures (*cf.* also **I**; *Sect. 3*).

Table 5. *Calculated Bond Lengths [Å] (bond orders) for the Molecules Used as Reference*

						
C(1)–C(2)	1.495(0.94)	1.494(0.96)	1.422(1.12)	1.082(0.89)	–	–
C(2)–C(3)	1.332(1.53)	1.403(1.05)	1.408(1.04)	1.330(0.96)	–	1.336(1.87)
C(2)–N(5)	1.446(0.83)	1.373(1.08)	1.500(0.77)	1.462(0.81)	–	–
C(3)–N(4)	1.227(1.88)	1.192(2.64)	1.185(2.36)	–	1.282(1.85)	–



N(1)–C(2)	1.267(1.86)
C(2)–C(3)	1.486(0.96)
C(2)–N(6)	1.364(1.08)
C(3)–C(4)	1.364(1.32)
C(3)–N(7)	1.407(0.92)
C(4)–N(5)	1.145(2.21)
N(5)–C(13)	1.392(0.78)

<sup>a)</sup> The same numbering of the atoms is used for all the structures.

Table 6. Calculated Charge Distributions [e] for Various Substitution Patterns of the Molecules (cf. Tables 4 and 5)

R = H, NH<sub>2</sub>, NO<sub>2</sub>  
X = C(NH)NH<sub>2</sub>, CH<sub>3</sub>

III

R	Charges			
	NO <sub>2</sub>	NH <sub>2</sub>	H	H <sup>a</sup> )
X	0.031	-0.023	-0.016	0.027
Y	0.360	0.155	-0.196	-0.221
R	-0.392	-0.131	0.212	0.195
μ [D]	2.8	2.7	2.1	1.8

<sup>a</sup>) X = CH<sub>3</sub>.

Depending on the nature of R in **III** (Table 6), charge displacements up to 0.6 e between the fragment Y and the substituent R are induced. Surprisingly, the total charge of the fragment X is extraordinarily stable (max. fluctuation 0.06 e). The nature of R influences the bond lengths and bond orders in X = CNH(NH<sub>2</sub>) very little. The X–Y bond is a single bond, and, although both fragments possess an almost coplanar π-system, no increase in the bond order is detected. The bond Y–R is also a single bond with little bond-order variation upon changing R. The bond order of Y–R is lower than that of X–Y, reaching its lowest value for R = NO<sub>2</sub>. The C,N bond in Y is a double bond for R = H, NH<sub>2</sub> increasing its bond order by ca. 5% for R = NO<sub>2</sub>. These results did not support a large contribution from a mesomeric structure of type **II**.

In contrast to the C=N bond, the C=C bond in Y is highly dependent on the substituent R (Table 4). The bond order of the C=C bond in methylketene imine (X = Me, R = H; cf. Table 4) is ca. 5% lower than in ethylene (cf. Table 4). In the amidinoketene imine (X = CNH(NH<sub>2</sub>), R = H; cf. Table 4), it decreases by a further 6% reaching the value 1.65, which represent 94% of the methylketene-imine value and 88% of that of ethylene. In the series of amidinoketene imines with R = H, NH<sub>2</sub>, NO<sub>2</sub>, the bond order of the C=C bond in Y remarkably drops from 1.65 (94%) to 1.55 (89%) and 1.43 (82%).

Based on the atomic net charges, the charge displacement Y → R as a function of R reveals that the charge is mainly taken from C(3), while only a little flows from the C=NH group to the R substituent (Table 6). Thus, replacing R = H by R = NO<sub>2</sub> causes a charge displacement from C(3) to R of ca. 0.46 e, which corresponds to 77% of the total charge displacement to the NO<sub>2</sub> group; 8% are coming from X = CNH(NH<sub>2</sub>) and 15% from the C=NH bond. This is in accordance with the differences found between ethylene and nitroethylene though the C=C bond order decreases there by only 4% (Table 5).

**4. Discussion.** – Ketene imines of type **1** were reported to react with aliphatic and aromatic amines affording amidines in good yields [37][38]. Likewise, Goerdeler *et al.*

isolated from the reaction of aniline with unstable alkene-diimines, formed by S-extrusion from isothiazolimines, amidine derivatives which allowed the indirect determination of the yields of formed ketene imines [5][28]. In accordance with these results, the presence of amines in the reaction mixture, as well as addition of amine after the completed desulfurization of 4-nitroisothiazol-5(2*H*)-imine **3**, led to amidine derivatives **5** in good yields (*Scheme 2* and *Table 1*). Therefore, also in this case, the presence of an unstable intermediate **A** as the main product of the reaction can be postulated. Surprisingly, neither aniline nor substituted anilines yielded the expected amidines, and the reaction proceeded as in the absence of amines yielding decomposition compounds and the *N*-oxide **4** as a minor product [32].

Following the discussion of the reactivity of amines in the reaction with ketene imines by *Stevens et al.* [37], we tried to correlate the reaction capability with the  $pK_a$  values of the used amines (*Table 7*). Thus, only relatively basic amines ( $pK_a > 8$ ) reacted with the intermediate **A** to yield the expected amidine derivatives; 4-methoxyaniline ( $pK_a = 5.29$ ) and aniline ( $pK_a = 4.62$ ) failed to react, in analogy with the results for some other ketene imines [5][37]. Steric hindrance as the inhibiting factor in these reactions was ruled out, as the expected derivatives from the reactions of **A** with  $\text{PhCH}_2\text{NH}_2$  and  $\text{PhSH}$  could be isolated (*cf. Table 1* and *Scheme 2*).

Table 7.  $pK_a$  Values of the Compounds Used as Trapping Reagents

Compound	$pK_a^a$	Compound	$pK_a$
Pyrrolidine	11.27	i-PrSH	10.86
$\text{Et}_2\text{NH}$	10.98	PrSH	10.82
$\text{EtNH}_2$	10.63	BuSH	10.78
$\text{PhCH}_2\text{NH}_2$	9.34	PhSH	6.50
Morpholine	8.36	MeOH	16.60
4-Methoxyaniline	5.29	4-Nitrophenol	7.14
$\text{PhNH}_2$	4.62	PhCOSH	5.66
		PhCOOH	4.20

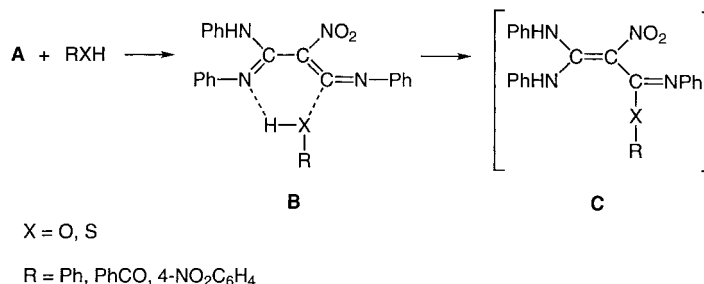
<sup>a</sup>)  $pK_a$  Values of the ammonium salt.

In contrast to the results with the amines, the reactions with thiols yielded the predicted adduct **6** only in the case of  $\text{PhSH}$  ( $pK_a = 6.50$ ). The less acidic ( $pK_a > 10$ ) *i*-PrSH, PrSH, and BuSH did not lead to any product, and again the reaction behavior was similar to that in the absence of nucleophiles. Whereas identical results were achieved when MeOH ( $pK_a = 16.60$ ) was used as reagent or as solvent, the addition of the more acidic 4-nitrophenol ( $pK_a = 7.14$ ) affected the reaction course as amines did. It should be noted, however, that the presumably formed primary adduct **9** decomposed during workup, and only the observed reaction behavior and the analysis of the crude product by mass spectrometry gave evidence of its formation. Furthermore, the addition of PhCOOH ( $pK_a = 4.20$ ) as well as PhCOSH ( $pK_a = 5.66$ ), after desulfurization of **3**, yielded products which would involve, as precursors, the expected adducts of the acids with intermediate **A** (*Schemes 3* and *4*).

Accordingly, ketene imines are known to add carboxylic acids giving enol esters, which are used as acylating agents. Their formation was explained *via* an intermediate acid/ketene imine adduct, which undergoes spontaneous intramolecular acyl migration

[39–41]. Mechanistic studies have shown that the driving force of this reaction is the affinity of the acid proton to the ketene imine; the stronger the acid, the faster the reaction [42]. Taking these results into account, one could propose a mechanism for the reaction of **A** with acidic reagents which involves the formation of a transition state **B** leading to the unstable adduct **C** (Scheme 6).

Scheme 6



In the case of  $\text{PhCOOH}$ , we assume that **C** (cf. **7a**, Scheme 3) possesses a favorable geometry for an easy  $O,N$ -acyl migration, similar to that observed for the addition products of amines and ketene imines [38]. In contrast, in the adduct **C** of  $\text{PhCOSH}$  and **A** (cf. **8a**, Scheme 4), the large  $\text{S}$ -atom might induce a different geometry, which apparently hinders the intramolecular acylation facilitating the hydrolysis of the unstable **C**. A diverging feature of the  $O,N$ - and  $S,N$ -acyl migrations is also the large energy difference of the products (2  $\text{C}=\text{O}$  vs.  $\text{C}=\text{O}$  and  $\text{C}=\text{S}$ ). Therefore, an early  $\text{TS}^\ddagger$  is to be expected in the first case and a late  $\text{TS}^\ddagger$  in the second case.

In summary, it seems that not only the nucleophilicity but also the acidity of the reagent is dominant in the reaction of nucleophiles with **A**. By examination of the results, one could ascertain the  $\text{p}K_a$  influences of different nucleophiles on this reaction. Whereas the increase in the basicity is proportional to the nucleophilicity and, therefore, to the reaction ability within the series of the amines, the effect for acidic compounds is the opposite. This becomes understandable considering the proposed mechanism, where the release of the acidic  $\text{H}$ -atom would favor the nucleophilic addition. Thus, in contrast to the other thiols, the acidity of  $\text{PhSH}$ , in addition to the stabilizing effect of the  $\text{Ph}$  ring on the formed anion, probably promotes the attack of the  $\text{S}$ -atom at the electrophilic  $\text{C}$ -atom of the ketene imine; analogously, 4-nitrophenol led to reaction while  $\text{MeOH}$  failed.

Interestingly, the two IR bands at  $2337$  and  $2261 \text{ cm}^{-1}$  of the reaction mixture of the desulfurization of **3** disappeared instantaneously when the solutions were treated with the nucleophiles. The isolated products could arise only from the addition of the reagents to the proposed ketene imine **A** and, therefore, the amidine derivatives **5**, the thioimidate **6**, the amide **7**, and the thioamide **8** undoubtedly establish that **A** is the unstable intermediate of the reaction. The shift of the IR bands compared with those of typical ketene imines (*ca.*  $2000 \text{ cm}^{-1}$ ) could be explained by the influence of the  $\text{NO}_2$  group which might give rise, due to its strong electron-withdrawing effect, to changes of the electronic characteristic of the cumulene. In fact, the *ab initio* calculations indicate

that 3-imino-2-nitroprop-2-enamidines are conveniently described by the single structure **I** (*cf. Sect. 3*); on the other hand, two further resonance structures, one of those analogous to the polar resonance form **II**, contribute significantly to the ground state of simple ketene imines of type **1** [43]. Theoretical studies and crystal structure analyses of those ketene imines [44][45] further support the contribution of the structure **II**, showing an increase of the C=N bond order depending on the substituents.

Taking into account the extent of the contribution of the resonance structures to their ground state, the reactivity differences between other 3-imino-2-nitroprop-2-enamidines of type **A** and ketene imines could be explained. Thus, ketene imines are reported to react not only as electrophiles at the central C-atom but also as nucleophiles at the terminal C-atom [12]. In contrast, the results of the calculations for **I** display a decrease of the nucleophilicity of the terminal C-atom, as the charge displacement to the NO<sub>2</sub> group is mainly taken from this C-atom (*cf. C(3) in I, Sect. 3*).

The formation of the 1,2,4-oxadiazole derivative<sup>7)</sup> **10** confirmed, on one hand, the electrophilic character of the ketene-imine C(3)-atom and showed, on the other hand, the participation of the NO<sub>2</sub> group in the reaction, as also achieved in the absence of nucleophiles as trapping reagents [32]. The proposed reaction mechanism could explain the different behavior of **A** and similar ketene imines, which typically undergo cycloadditions with phenyl isothiocyanate and phenyl isocyanate, while **A** failed to react. Probably, in **A**, where the electronic effects cause a high reactivity in the molecule, the O-atoms of the NO<sub>2</sub> group can easily reach the electrophilic C(2)-atom of the cumulene. This, together with several reactive sites of **A**, could induce many parallel reactions, thus leading to numerous decomposition compounds (*cf. [32]*). Nevertheless, the addition of strong nucleophiles as trapping reagents to the reaction mixture allows a ready blocking of the electrophilic C(2)-atom yielding stable adducts as proof for the appearance of the transient 3-imino-2-nitroprop-2-enamidine **A**.

We thank the analytical units of our institute for spectra and analyses. Financial support of this work by the Swiss National Science Foundation and F. Hoffmann-La Roche AG, Basel, is gratefully acknowledged. D.M.A. thanks the Eidgenössische Stipendienkommission für ausländische Studierende for a scholarship.

### Experimental Part

1. *General.* TLC: silica-gel 60-*F*<sub>254</sub> plates (0.25 mm; *Merck*); CH<sub>2</sub>Cl<sub>2</sub>/hexane 6 : 1, CH<sub>2</sub>Cl<sub>2</sub>/MeOH 20 : 1, and 100 : 1 as eluents. Column chromatography (CC): silica gel 60 (0.040–0.063 mesh; *Merck*). Medium-pressure liquid chromatography (MPLC): pump *LABOMATIC MD-80/100*, UV detector *LABOCORD-200* (254 nm); *LiChroprep Si 60* (*Merck*), 15–25 μm; column *Kronlab HPP-VPC*, 540 × 40 mm. Solvent: CH<sub>2</sub>Cl<sub>2</sub> (*puriss.*, abs., over molecular sieve; H<sub>2</sub>O < 0.005%; *Fluka*). M.p.: *Mettler-FP-5* apparatus, uncorrected. IR Spectra: *Perkin-Elmer-1600 FT-IR* spectrophotometer; in KBr, absorption bands in cm<sup>-1</sup>. <sup>1</sup>H- (300 or 600 MHz) and <sup>13</sup>C-NMR (75.5 or 150.9 MHz) Spectra: *Bruker ARX-300* and *Bruker AMX-600* instrument, in CDCl<sub>3</sub> unless otherwise stated; δ in ppm; coupling constants *J* in Hz. Signal multiplicity was indirectly interpreted from the DEPT spectra and signal assignment was achieved using 2D-NMR correlation spectra. CI-MS (NH<sub>3</sub> as ionization gas): *Finnigan SSQ-700* or *MAT-90* instrument; ESI mode on a *Finnigan TSQ-700* triple quadrupole spectrometer.

2. *Starting Material.* 4-Nitro-N,2-diphenyl-3-(phenylamino)isothiazol-5(2H)-imine (**3**) was synthesized according to the general procedure described in [30][47].

<sup>7)</sup> The synthesis of similar 1,2,4-oxadiazole derivatives starting from 4-nitroimidazoles have been described by *Suwinski et al.* [46], though *via* a different reaction mechanism involving reduction of the NO<sub>2</sub> to a NO group.

3. 2-Nitro-N-phenyl-3,3-bis(phenylamino)prop-2-enamides **5**. *General Procedure. Method A*: To a soln. of **3** (0.5 mmol) in abs. CH<sub>2</sub>Cl<sub>2</sub> (4 ml), containing the corresponding amine (5 mmol), a soln. of Ph<sub>3</sub>P (136 mg, 0.5 mmol) in abs. CH<sub>2</sub>Cl<sub>2</sub> (1.5 ml) was added at 0° under N<sub>2</sub>. The mixture was stirred for 1 h raising the temp. to r.t., then, the solvent was evaporated, and the residue separated by CC (CH<sub>2</sub>Cl<sub>2</sub>/MeOH). The compounds were purified by repeated CC.

*Method B*: To a soln. of **3** (0.5 mmol) in abs. CH<sub>2</sub>Cl<sub>2</sub> (4 ml), a soln. of Ph<sub>3</sub>P (136 mg, 0.5 mmol) in abs. CH<sub>2</sub>Cl<sub>2</sub> (1.5 ml) was added at 0° under N<sub>2</sub>. After 2 min, the desulfurization was completed (monitoring by TLC and IR), and the corresponding amine (5 mmol) was added. Workup and purification as in *Method A*.

3.1. 1-Morpholino-2-nitro-N-phenyl-3,3-bis(phenylamino)prop-2-enimine (**5a**). CC with CH<sub>2</sub>Cl<sub>2</sub>/MeOH. Yield of **5a**: 226 mg (99%, *Method A*), 205 mg (90%, *Method B*). Yellow crystals. M.p. 113–115°. IR: 3364w, 3239m, 3056m, 2962m, 2920m, 2856m, 1584s, 1525s, 1496s, 1439s, 1353s, 1278s, 1243s, 1204s, 1112s, 1061s, 1021m, 1002m, 944w, 912w, 855w, 810w, 751s, 722w, 692s. <sup>1</sup>H-NMR: 11.82 (br. s, 2 NH); 7.19 (t, J = 7.8, 2 arom. H); 7.0–6.7 (m, 9 arom. H); 6.48 (br. s, 4 arom. H); 3.69 (br. s, 2 CH<sub>2</sub>O); 3.55 (br. s, 2 CH<sub>2</sub>N). <sup>13</sup>C-NMR: 150.9 (s, C(3)); 150.6 (s, C(1)); 148.9 (s, 1 arom. C); 134.8 (br. s, 2 arom. C); 128.0, 127.8, 125.2, 122.5, 121.9, 120.5 (6d, 15 arom. CH); 107.9 (s, C(2)); 65.6 (br. t, 2 CH<sub>2</sub>O); 45.0 (br. t, 2 CH<sub>2</sub>N). ESI-MS: 466 ([M + Na]<sup>+</sup>), 444 ([M + H]<sup>+</sup>). Anal. calc. for C<sub>25</sub>H<sub>25</sub>N<sub>5</sub>O<sub>3</sub> (443.51): C 67.70, H 5.68, N 15.79; found: C 67.89, H 5.69, N 15.53.

3.2. 2-Nitro-N-phenyl-3,3-bis(phenylamino)-1-(pyrrolidin-1-yl)prop-2-enimine (**5b**). CC with CH<sub>2</sub>Cl<sub>2</sub>/MeOH. Yield of **5b**: 205 mg (93%, *Method A*); 158 mg (72%, *Method B*). Yellow crystals. M.p. 117–119°. IR: 3422w (br.), 3157m, 3053m, 2974m, 2867m, 1622s, 1586s, 1535s, 1496s, 1442s, 1350s, 1261s, 1227s, 1204s, 1143m, 1120m, 1098m, 1072m, 998w, 942m, 917m, 844w, 754s, 693s. <sup>1</sup>H-NMR ((D<sub>6</sub>)DMSO, 363 K): 9.38 (br. s, 2 NH); 7.29 (t, J = 7.5, 2 arom. H); 7.2–7.0 (m, 7 arom. H); 6.9–6.7 (m, 6 arom. H); 3.34 (m, 2 CH<sub>2</sub>N); 1.83 (m, 2 CH<sub>2</sub>). <sup>13</sup>C-NMR ((D<sub>6</sub>)DMSO, 363 K): 154.3 (s, C(3)); 148.2 (br. s, C(1)); 142.6, 140.5 (2 br. s, 3 arom. C); 127.9, 127.4, 124.2, 122.3, 121.5, 120.6 (6d, 15 arom. CH); 109.1 (s, C(2)); 48.0 (t, 2 CH<sub>2</sub>N); 23.6 (t, 2 CH<sub>2</sub>). ESI-MS: 428 ([M + H]<sup>+</sup>). Anal. calc. for C<sub>25</sub>H<sub>25</sub>N<sub>5</sub>O<sub>2</sub> (427.51): C 70.24, H 5.89, N 16.38; found: C 69.99, H 6.06, N 16.16.

3.3. N<sup>1</sup>,N<sup>1</sup>-Diethyl-2-nitro-N<sup>2</sup>-phenyl-3,3-bis(phenylamino)prop-2-enamide (**5c**). CC with CH<sub>2</sub>Cl<sub>2</sub>/MeOH. Yield of **5c**: 201 mg (91%, *Method A*). Yellow crystals. M.p. 170–173°. IR: 3356w, 3156m, 3056m, 2973m, 2931m, 1625s, 1582s, 1517s, 1497s, 1446s, 1356s, 1297m, 1262s, 1230s, 1208s, 1178m, 1091s, 1058s, 998w, 917m, 896m, 876w, 844w, 803w, 752s, 693s. <sup>1</sup>H-NMR: 11.92 (br. s, 2 NH); 7.20 (t, J = 7.8, 2 arom. H); 7.0–6.7 (m, 9 arom. H); 6.6–6.2 (br. m, 4 arom. H); 3.31 (br. s, 2 CH<sub>2</sub>); 1.18 (br. s, 2 Me). <sup>13</sup>C-NMR: 150.6 (s, C(3)); 150.0 (s, C(1)); 149.0 (s, 1 arom. C); 135.2 (br. s, 2 arom. C); 128.0, 127.6, 124.7, 122.7 (br.), 121.6, 120.7, (6d, 15 arom. CH); 109.3 (s, C(2)); 42.4, 40.7 (2br. t, 2 CH<sub>2</sub>); 14.3, 11.0, (2br. q, 2 Me). ESI-MS: 430 ([M + H]<sup>+</sup>). Anal. calc. for C<sub>25</sub>H<sub>27</sub>N<sub>5</sub>O<sub>2</sub> (429.52): C 69.91, H 6.34, N 16.31; found: C 69.80, H 6.04, N 16.51.

3.4. N<sup>1</sup>-Benzyl-2-nitro-N<sup>2</sup>-phenyl-3,3-bis(phenylamino)prop-2-enamide (**5d**). CC with CH<sub>2</sub>Cl<sub>2</sub>/MeOH. Yield of **5d**: 172 mg (76%<sup>8</sup>), *Method A*). Yellow crystals. M.p. 91–93°. IR: 3366m, 3288m, 3057m, 1611s, 1587s, 1539s, 1496s, 1441s, 1356s, 1217s, 1123m, 1073s, 1028m, 999w, 913w, 752s, 693s. <sup>1</sup>H-NMR ((D<sub>6</sub>)DMSO): 10.08 (br. s, 1 NH); 9.14 (br. s, 2 NH); 7.8–6.6 (m, 15 arom. H); 4.14 (br. s, CH<sub>2</sub>). <sup>13</sup>C-NMR ((D<sub>6</sub>)DMSO): 154.7 (br., C(3)); 150.8 (br. s, C(1)); 147.1, 138.0 (2br. s, 2 arom. C); 137.0 (s, 2 arom. C); 128.4, 128.1, 127.3, 127.0, 124.7, 123.1, 121.6 (br.), 119.2 (br.) (8d, 20 arom. CH); 111.0 (s, C(2)); 46.8 (t, CH<sub>2</sub>). ESI-MS: 927 ([2M + H]<sup>+</sup>), 486 ([M + Na]<sup>+</sup>), 464 ([M + H]<sup>+</sup>). Anal. calc. for C<sub>28</sub>H<sub>25</sub>N<sub>5</sub>O<sub>2</sub> (463.54): C 72.55, H 5.44, N 15.11; found: C 72.52, H 5.27, N 15.15.

4. Phenyl 2-Nitro-N-phenyl-3,3-bis(phenylamino)prop-2-enethioimidate (**6**). According to the *General Procedure, Method B* (cf. 3), PhSH (0.5 ml, 5.2 mmol) was added after desulfurization of **3**. CC with CH<sub>2</sub>Cl<sub>2</sub>/MeOH. Yield of **6**: 149 mg (62%). Yellow crystals. M.p. 140–141° (dec.). IR: 3278w (br.), 3054m, 2956w, 2922w, 2867w, 1611s, 1594s, 1583s, 1521s, 1497s, 1480s, 1460s, 1440s, 1400s, 1351s, 1286s, 1239m, 1222s, 1207s, 1172m, 1156m, 1067s, 1025m, 1000w, 948m, 922m, 905m, 879m, 847w, 770m, 752s, 743s, 700s, 691s. <sup>1</sup>H-NMR: 10.40 (br. s, 2 NH); 7.5–6.8 (m, 20 arom. H). <sup>13</sup>C-NMR: 163.7 (s, C(1)); 150.4 (s, C(3)); 148.3, 136.4 (2s, 3 arom. C); 135.3 (d, 2 arom. CH); 130.0 (s, 1 arom. C); 129.4, 129.2, 128.9, 128.8, 128.7, 125.5, 122.1, 120.3, (8d, 18 arom. CH); 115.2 (s, C(2)). ESI-MS: 467 ([M + H]<sup>+</sup>). Anal. calc. for C<sub>27</sub>H<sub>22</sub>N<sub>4</sub>O<sub>2</sub>S (466.56): C 69.51, H 4.75, N 12.01; found: C 69.29, H 4.85, N 12.00.

5. N-[2-Nitro-1-(phenylamino)-2-(N-phenylcarbamoyl)ethenyl]-N-phenylbenzamide (**7**). According to the *General Procedure, Method B* (cf. 3), PhCOOH (635 mg, 5.2 mmol) was added after desulfurization of **3**. CC with CH<sub>2</sub>Cl<sub>2</sub>/MeOH. Yield of **7**: 165 mg (67%). Yellow crystals. M.p. 104–106° (dec.). IR: 3303m, 3061m,

<sup>8</sup>) The yield of the reaction may be higher, but the isolation of the compound was particularly difficult.



2924w, 1672s, 1581s, 1538s, 1483s, 1445s, 1403m, 1334s, 1285s, 1179m, 1140m, 1101m, 1075m, 1049m, 1027w, 1002w, 889m, 864w, 786m, 756s, 722m, 691s. <sup>1</sup>H-NMR (CD<sub>3</sub>CN, 220 K): 11.29, 9.11 (2s, 2 NH); 7.7–6.5 (m, 20 arom. H). <sup>13</sup>C-NMR (CD<sub>3</sub>CN, 220 K): 172.0 (s, C=O); 159.2 (s, (PhNH)<sub>2</sub>C); 154.2 (s, C=O); 139.7, 138.7, 135.8, 133.5 (4s, 4 arom. C); 132.4, 129.8, 129.7, 129.3, 129.2, 128.9, 128.7, 128.4, 127.2, 125.5, 124.7 (11d, 18 arom. CH); 123.2 (s, NO<sub>2</sub>C); 119.1 (d, 2 arom. CH). ESI-MS: 501 ([M+Na]<sup>+</sup>), 479 ([M+H]<sup>+</sup>).

6. 2-Nitro-N-phenyl-3,3-bis(phenylamino)prop-2-enethioamide (**8**)<sup>9</sup>. According to the *General Procedure, Method B* (cf. 3), PhCOSH (635 mg, 5.2 mmol) was added after desulfurization of **3**. CC with CH<sub>2</sub>Cl<sub>2</sub>/MeOH. Yield of **8** (cf. [34]): 150 mg (75%). ESI-MS: 391 ([M+H]<sup>+</sup>), 389 ([M-H]<sup>+</sup>)<sup>10</sup>.

7. 4-Nitrophenyl 2-Nitro-N-phenyl-3,3-bis(phenylamino)prop-2-enimidate (**9**). According to the *General Procedure, Method B* (cf. 3), 4-nitrophenol (723 mg, 5.2 mmol) was added after desulfurization of **3**. CC with CH<sub>2</sub>Cl<sub>2</sub>/MeOH<sup>11</sup>). ESI-MS: 496 ([M+H]<sup>+</sup>).

8. 4,5-Dihydro-4-methyl-N',N<sup>2</sup>,5-triphenyl-1,2,4-oxadiazole-3-carbamidine (**10**). According to the *General Procedure, Method A* (cf. 3), in presence of 0.6 ml (5.2 mmol) of (benzylidene)(methyl)amine. CC with CH<sub>2</sub>Cl<sub>2</sub>/MeOH and MPLC with CH<sub>2</sub>Cl<sub>2</sub>/hexane. Yield of **10**: 42.7 mg (36%). White crystals. M.p. 169–170°. IR: 3295m, 3136m, 3060m, 2923m, 2854w, 2804w, 1641s, 1590s, 1549s, 1483s, 1477s, 1446s, 1409m, 1372m, 1328s, 1290m, 1218s, 1176w, 1156w, 1118m, 1072m, 1016m, 901w, 830m, 758s, 697s. <sup>1</sup>H-NMR (CD<sub>2</sub>Cl<sub>2</sub>, 208 K): 7.76 (d, J = 7.9, 2 arom. H); 7.46 (br. s, 1 NH); 7.4–7.3 (m, 5 arom. H); 7.28 (t, J = 7.5, 2 arom. H); 7.16 (t, J = 7.4, 1 arom. H); 7.09 (t, J = 7.4, 1 arom. H); 7.01 (d, J = 7.5, 2 arom. H); 6.89 (d, J = 7.3, 2 arom. H); 5.94 (s, CH); 2.30 (s, Me). <sup>13</sup>C-NMR (CD<sub>2</sub>Cl<sub>2</sub>, 208 K): 153.3 (s, C(3)); 148.2 (s, 1 arom. C); 140.4 (s, (NH)C=N); 138.8, 135.4 (2s, 2 arom. C); 130.0, 128.9, 128.8, 128.5, 127.6, 123.5, 123.2, 121.0, 119.3 (9d, 15 arom. CH); 99.0 (d, C(5)); 31.5 (q, Me). ESI-MS: 735 ([2M+Na]<sup>+</sup>), 379 ([M+Na]<sup>+</sup>), 357 ([M+H]<sup>+</sup>). Anal. calc. for C<sub>22</sub>H<sub>20</sub>N<sub>4</sub>O (356.43): C 74.14, H 5.66, N 15.72; found: C 74.08, H 5.47, N 15.36.

9. *Crystal-Structure Determination of 8 and 10* (see Table 8, and Figs. 1 and 2)<sup>12</sup>. All measurements were made on a Rigaku-AFC5R diffractometer using graphite-monochromated MoK<sub>α</sub> radiation (λ = 0.71069 Å) and a 12-kW rotating anode generator. The ω/2θ scan mode was employed for data collection. The intensities were corrected for Lorentz and polarization effects, but not for absorption. Data collection and refinement parameters are given in Table 8, views of the molecules are shown in Figs. 1 and 2. The structures were solved by direct methods using SHELXS86 [48], which revealed the positions of all non-H-atoms. The asymmetric unit of **8** contains two symmetry-independent molecules plus a partially occupied site for a H<sub>2</sub>O molecule. The mol-% of H<sub>2</sub>O is ca. 10%. In the asymmetric unit of **10**, there are also two symmetry-independent molecules. The atomic coordinates of the two molecules were tested carefully for a relationship from a higher symmetry space group using the MISSYM routine [49] of the program PLATON [50], but none could be found. The non-H-atoms of **8** and **10** were refined anisotropically. All of the H-atoms bonded to N-atoms were placed in the positions indicated by a difference electron-density map and their positions were allowed to refine together with individual isotropic displacement parameters. The H-atoms of H<sub>2</sub>O in **8** were similarly located, but not refined. All remaining H-atoms were fixed in geometrically calculated positions (d(C–H) = 0.95 Å), and they were assigned fixed isotropic displacement parameters with a value equal to 1.2 U<sub>eq</sub> of the parent C-atom. Refinement of the structures was carried out on F using full-matrix least-squares procedures, which minimized the function Σw(|F<sub>o</sub> – |F<sub>c</sub>||)<sup>2</sup>. Neutral atom scattering factors for non-H-atoms were taken from [51a] and the scattering factors for H-atoms from [52]. Anomalous dispersion effects were included in F<sub>calc</sub>. [53]; the values for f' and f'' were those of [51b]. All calculations were performed using the TEXSAN crystallographic software package [54].

<sup>9</sup>) The expected adduct could not be isolated, only the product of its hydrolysis.

<sup>10</sup>) Usually observed peak in the MS spectra of thioacrylamides of this series.

<sup>11</sup>) According to TLC, only one main product has been formed in the reaction, but it decomposed to undefined compounds during flash chromatography. However, the MS of an isolated impure fraction indicated the desired adduct.

<sup>12</sup>) Crystallographic data (excluding structure factors) for the structures reported in this paper have been deposited with the Cambridge Crystallographic Data Centre as deposition No. CCDC-104936 and 104937 for **8** and **10**, resp. Copies of the data can be obtained, free of charge, on application to the CCDC, 12 Union Road, Cambridge CB2 1EZ, U.K. (fax: +44-(0)1223-336033 or e-mail: deposit@ccdc.cam.ac.uk).

Table 8. Crystallographic Data for Compounds **8** and **10**

	<b>8</b>	<b>10</b>
Crystallized from	MeOH	MeOH
Empirical formula	C <sub>21</sub> H <sub>18</sub> N <sub>4</sub> O <sub>2</sub> S · 0.1 H <sub>2</sub> O	C <sub>22</sub> H <sub>20</sub> N <sub>4</sub> O
Formula weight	392.26	356.43
Crystal color, habit	yellow, tablet	colorless, prism
Crystal dimensions [mm]	0.12 × 0.23 × 0.45	0.10 × 0.25 × 0.33
Temperature [K]	173(1)	173(1)
Crystal system	monoclinic	monoclinic
Space group	<i>P</i> 2 <sub>1</sub> / <i>n</i>	<i>P</i> 2 <sub>1</sub>
<i>Z</i>	8	4
Reflections for cell determination	25	25
2 $\theta$ Range for cell determination [°]	24–39	26–39
Unit cell parameters <i>a</i> [Å]	13.272(3)	7.336(5)
<i>b</i> [Å]	15.687(4)	20.981(3)
<i>c</i> [Å]	19.045(2)	12.706(5)
$\beta$ [°]	93.93(1)	90.96(4)
<i>V</i> [Å <sup>3</sup> ]	3956(1)	1955(2)
<i>D</i> <sub>calc</sub> [g cm <sup>-3</sup> ]	1.317	1.211
$\mu$ (MoK $\alpha$ ) [mm <sup>-1</sup> ]	0.188	0.0769
2 $\theta$ (max) [°]	50	55
Total reflections measured	7584	4962
Symmetry independent reflections	6971	4605
Reflections used [ <i>I</i> > 2 $\sigma$ ( <i>I</i> )]	4114	2602
Parameters refined	538	495
Final <i>R</i>	0.0521	0.0516
<i>wR</i> ( <i>w</i> = [ $\sigma^2(F_o) + (0.005F_o)^2$ ] <sup>-1</sup> )	0.0422	0.0370
Goodness of fit	1.585	1.377
Secondary extinction coefficient	–	4.7(8) × 10 <sup>-7</sup>
Final $\Delta_{\max}/\sigma$	0.0003	0.0002
$\Delta\rho$ (max; min) [e Å <sup>-3</sup> ]	0.26; –0.26	0.21; –0.20

## REFERENCES

- [1] A. F. Khlebnikov, M. S. Novikov, R. R. Kostikov, *J. Org. Chem. USSR (Engl. Transl.)* **1989**, 25, 2103.
- [2] M. P. Wentland, P. E. Hansen, S. R. Schow, S. J. Daum, *Tetrahedron Lett.* **1989**, 30, 6619.
- [3] K. Araki, J. A. Wichtowski, J. T. Welch, *Tetrahedron Lett.* **1991**, 32, 5461.
- [4] E. Schaumann, S. Grabley, *Liebigs Ann. Chem.* **1981**, 290.
- [5] J. Goerdeler, A. Laqua, C. Lindner, *Chem. Ber.* **1980**, 113, 2509.
- [6] L. Capuano, P. Mörsdorf, H. Scheidt, *Chem. Ber.* **1983**, 116, 741.
- [7] L. Capuano, B. Dahm, V. Port, R. Schnur, V. Schramm, *Chem. Ber.* **1988**, 121, 271.
- [8] Y. Nagao, T. Kumagai, S. Takao, T. Abe, M. Ochiai, *J. Org. Chem.* **1986**, 51, 4739.
- [9] G. Barbaro, A. Battaglia, P. Giorgianni, D. Giacomini, *Tetrahedron* **1993**, 49, 4293.
- [10] P. Carisi, G. Mazzanti, P. Zani, G. Barbaro, A. Battaglia, P. Giorgianni, *J. Chem. Soc., Perkin Trans. 1* **1987**, 2647.
- [11] P. Molina, M. Alajarin, A. Vidal, *J. Org. Chem.* **1991**, 56, 4008.
- [12] A. Dondoni, *Heterocycles* **1980**, 14, 1547.
- [13] D. Gröschl, H.-P. Niedermann, H. Meier, *Chem. Ber.* **1994**, 127, 955.
- [14] M. A. Walters, C. S. McDonough, P. S. Brown, A. B. Hoem, *Tetrahedron Lett.* **1991**, 32, 179.
- [15] P. Molina, M. Alajarin, C. Lopez-Leonardo, *Tetrahedron Lett.* **1991**, 32, 4041.
- [16] M. A. Walters, A. B. Hoem, H. R. Arcand, A. D. Hegeman, C. S. McDonough, *Tetrahedron Lett.* **1993**, 34, 1453.
- [17] H. Staudinger, E. Hauser, *Helv. Chim. Acta* **1921**, 4, 887.

- [18] G. R. Krow, *Angew. Chem.* **1971**, *83*, 455.
- [19] C. L. Stevens, G. H. Singhal, *J. Org. Chem.* **1963**, *29*, 34.
- [20] R. Fuks, D. Baudoux, *J. Org. Chem.* **1988**, *53*, 18.
- [21] R. Appel, R. Kleinstück, K.-D. Ziehn, *Chem. Ber.* **1971**, *104*, 1335.
- [22] J. Goerdeler, S. Raddatz, *Chem. Ber.* **1980**, *113*, 1095.
- [23] O. Mitsunobu, K. Kato, M. Wada, *Bull. Soc. Chem. Jpn.* **1971**, *44*, 1362.
- [24] J. Goerdeler, C. Lindner, *Chem. Ber.* **1980**, *113*, 2499.
- [25] J. Goerdeler, A. Laqua, C. Lindner, *Chem. Ber.* **1974**, *107*, 3518.
- [26] M. I. García Trimiño, A. Linden, H. Heimgartner, A. Macías Cabrera, *Helv. Chim. Acta* **1993**, *76*, 2817.
- [27] J. Goerdeler, M. Yunis, H. Puff, A. Roloff, *Chem. Ber.* **1986**, *119*, 162.
- [28] J. Goerdeler, J. Haag, C. Lindner, R. Losch, *Chem. Ber.* **1974**, *107*, 502.
- [29] J. Goerdeler, C. Lindner, F. Zander, *Chem. Ber.* **1981**, *114*, 536.
- [30] D. Moya Argilagos, M. I. García Trimiño, A. Macías Cabrera, A. Linden, H. Heimgartner, *Helv. Chim. Acta* **1997**, *80*, 273.
- [31] D. Moya Argilagos, R. W. Kunz, A. Linden, H. Heimgartner, *Chimia* **1997**, *51*, 455.
- [32] D. Moya Argilagos, A. Linden, H. Heimgartner, in preparation.
- [33] S. Rajappa, *Tetrahedron* **1981**, *37*, 1453.
- [34] D. Moya Argilagos, A. Macías Cabrera, M. I. García Trimiño, H. Vélez Castro, *Synth. Commun.* **1996**, *26*, 1187.
- [35] C. K. Johnson, 'ORTEPII, Report ORNL-5138', Oak Ridge National Laboratory, Oak Ridge, Tennessee, 1976.
- [36] J. Bernstein, R. E. Davis, L. Shimoni, N.-L. Chang, *Angew. Chem., Int. Ed. Engl.* **1995**, *34*, 1555.
- [37] C. L. Stevens, R. C. Freeman, K. Noll, *J. Org. Chem.* **1965**, *30*, 3718.
- [38] D. J. Woodman, Z. L. Murphy, *J. Org. Chem.* **1969**, *34*, 3451.
- [39] D. J. Woodman, R. A. Olofson, *J. Am. Chem. Soc.* **1961**, *83*, 1007.
- [40] D. J. Woodman, A. I. Davidson, *J. Org. Chem.* **1970**, *35*, 83.
- [41] D. J. Woodman, A. I. Davidson, *J. Org. Chem.* **1973**, *38*, 4288.
- [42] D. F. Mironova, N. A. Loginova, *J. Org. Chem. USSR (Engl. Transl.)* **1984**, *20*, 2344.
- [43] J. Firl, W. Runge, W. Hartmann, H.-P. Utikal, *Chem. Lett.* **1975**, 51.
- [44] H. W. Kroto, G. Y. Matti, R. J. Suffolk, J. D. Watts, M. Rittby, R. J. Bartlett, *J. Am. Chem. Soc.* **1990**, *112*, 3779.
- [45] J. Lambrecht, B. Gambke, J. von Seyerl, G. Huttner, G. Kollmannsberger-von Nell, S. Herzberger, J. C. Jochims, *Chem. Ber.* **1981**, *114*, 3751.
- [46] J. Suwinski, W. Pawlus, E. Salwinska, K. Swierczek, *Heterocycles* **1994**, *37*, 1511.
- [47] M. I. García Trimiño, D. Moya Argilagos, A. Macías Cabrera, A. Linden, H. Heimgartner, *Helv. Chim. Acta* **1998**, *81*, 718.
- [48] G. M. Sheldrick, SHELXS86, *Acta Crystallogr., Sect. A* **1990**, *46*, 467.
- [49] a) Y. LePage, *J. Appl. Crystallogr.* **1987**, *20*, 264; b) *ibid.* **1988**, *21*, 983.
- [50] A. L. Spek, *Acta Crystallogr., Sect. A* **1990**, *46*, C31.
- [51] a) E. N. Maslen, A. G. Fox, M. A. O'Keefe, in 'International Tables for Crystallography', Ed. A. J. C. Wilson, Kluwer Academic Publishers, Dordrecht, 1992, Vol. C, Table 6.1.1.1, p. 477; b) D. C. Creagh, W. J. McAuley, *ibid.*, Table 4.2.6.8, p. 219.
- [52] R. F. Stewart, E. R. Davidson, W. T. Simpson, *J. Chem. Phys.* **1965**, *42*, 3175.
- [53] J. A. Ibers, W. C. Hamilton, *Acta Crystallogr.* **1964**, *17*, 781.
- [54] TEXSAN Single Crystal Structure Analysis Software, Version 5.0. Molecular Structure Corporation, The Woodlands, Texas, 1989.

Received October 26, 1998